PINSA, **66, A,** No. 6, November 2000, pp. 653-674.
© Printed in India

HIGH ENERGY ACCELERATORS AND MATERIALS SCIENCE

G K MEHTA

Nuclear Science Centre, Aruna Asaf Ali Marg, New Delhi - 110 067 (India)

(Received 29 October 1999; Accepted 29 May 2000)

High energy ion beams are proving to be versatile tools for modification and depth profiling of materials. Swiftly moving ions in material interact predominantly with electrons through inelastic scattering and the other independent mode of interaction i.e. elastic scattering with nuclei has negligible contribution. This provides novel possibilities distinctly different than with low energy ions, of engineering the materials. Swift Heavy Ion (SHI) produces a column of a few tens of nm filled with ionized material. Depending upon the density of the electronic energy in the region and the properties of the material, the columnar region can relax back to original matter with no defects, or get series of point defects, clusters or a continuous track of amorphised material. These columns become continuous tracks in most materials beyond a threshold, which depends on the material properties, value of electronic energy density. These columnar tracks improve the properties of high temperature superconductors, produce nanostructures, synthesize novel materials etc. Electronic energy loss induced surface modification, sputtering, ion beam mixing are emerging areas with interesting physics and applications. Dynamic studies during irradiation and *in situ* surface studies are useful in understanding the ion-solid interactive process.

Key Words: High-Energy Ion Irradiation; Semiconductors; Ion Beam Mixing; HTSC; Electronic Sputtering; ERDA; Nanostructures

1 Introduction

Nuclear accelerators originally planned for basic nuclear and atomic physics research invariably open up completely new perspectives in various fields, particularly in materials science and device technology. Low energy accelerators are now standard tools and their exploitation in engineering materials of all kinds of interest: electronic, tribological, metallurgical etc. provide very fruitful activity. With the advances in technologies ion beams of almost all the elements across the periodic table are becoming accessible over a very wide range of energies. Heavy ion beams of energies upto hundreds of MeV are beginning to be exploited in almost all the emerging new areas in materials science.

Ions interact with matter through both electrons and nuclei. These interactions produce changes in the properties of the matter which may be desirable or detrimental. The best known application of ion beam is implantation in which a specific element is deposited within the structure of the material to modify the properties of the material in the implantation region. The placement of a foreign element in the material is often desirable, for example in semiconductor technology to produce n or p type materials. However, while the ion is slowing down to come to rest at its predetermined location adjusted by the energy of the ion (range), it causes some movement of lattice atoms from their sites, i.e. creates defects. The movement of lattice atoms is directly created by elastic collisions of the ions with the nuclei, a process which predominates at low energy. At higher energy ion interacts predominantly through inelastic collisions with electrons which normally does not affect the lattice unless the electronic energy loss in the material exceeds certain threshold value. This fact can make deep implantation a useful tool for devices. Defects created near the implantation region can be annealed. High energy ions can cause some dynamic annealing which can provide beneficial effects. Applications of ion beams always involve balance between the beneficial and detrimental effects of ion interaction with matter.

Ion implantation has always offered certain unique

possibilites for modification of all classes of materials. The energy range of ion-implanters is gradually increasing and MeV ion implantation machines for industrial use are now available. Novel treatments using novel implantation machines for industrial use are now available. Novel treatments using novel implantation procedures, e.g. ion beam mixing (IBM), ion beam assisted deposition (IBAD) have been invented. A large variety of applications have emerged and is expected to increase in future as the higher energy induced effects are understood.

Fast ions with energies greater than MeV/nucleon (MeV/u), called Swift Heavy Ions (SHI), are becoming increasingly important tools in many fields. The wide choice of ion species and energies allows features which makes them very versatile probes opening possibilities of engineering materials to fine tune some properties, tailoring the device characteristics, creating channels of modified refractive index material, producing nano-structures etc. SHI seems to be emerging as a very versatile tool for applications in diverse areas of materials sciences, sensors and devices.

This article is not an exhaustive review of this emerging area of swift heavy ions in materials engineering and characterization (SHIMEC). A brief introduction to the passage of swift heavy ions through the material is first given with an aim to bring to the focus the basic theme of electronic excitations produced by SHI and their role, which is distinctly different for nuclear collisions, in materials science. Impact of SHI in different types of materials and associated techniques is then described. Emphasis is given to the subjects investigated by the users of the Pelletron facility at the Nuclear Science Centre. Efffort is made to cover the work in these areas in other laboratories.

2 Heavy Ions in Materials Science

An energetic charged particle moving in a solid loses energy through various processes and if it is a heavy ion, it picks up electrons into various shells as its velocity passes successively through the orbital velocities of those shells. Ultimately, a very slowly moving ion propagates almost as a neutral atom going through cascade of collisions and stops in the solid. The role of heavy ions in materials science can be separated in four regimes:

Atomic Regime (<keV/u>)

In this low energy (keV per nucleon) regime, the elastic scattering with nuclei results in kinematic transfer of energy by the heavy ion to atom leading to collision cascades and sputtering. Ions lose energy by elastic collisions upto a point. When the energy is too low to dislodge atoms from their site they excite phonons and finally the ions come to rest i.e. get implanted. Ion implantation is now being done at higher energies to get buried implants. High energy is just to go deeper in the material but the implantation is, of course, low energy phenomenon. Low energy ion bombardment of surfaces is an excellent way for surface cleaning, ion etching.

Electronic Regime (~1MeV/u)

The energy loss in this energy region is predominantly through inelastic scattering to electrons. This energy locked in the electron excitations gets coupled to the lattice and is responsible for interesting phenomena observed in the materials when heavy ions pass through them. The electron excitations give rise to the generation of characteristic X-rays. Proton Induced X-ray Emission Analysis (PIXEA) is a technique which has given rise to a very sensitive method for non-destructive trace element analysis to a level of 0.1ppm and with some efforts can be taken to a level upto 1ppb. Heavy Ion Induced X-ray Emission (HIXE) provides very sensitive technique for special cases where only a few elements are involved as it gives rise to complicated spectra if multi-elements are present.

Elastic Regime

For materials science applications we have to ensure that there are no nuclear reactions occurring inside the sample, except when required for specific element connected technique using nuclear reactions. Thus the energy of heavy ions is kept below the Coulomb barrier to ensure that impinging ions cannot approach the nuclei of the materials close enough to see their nuclear interaction. In other words, only scattering due to the Coulomb field takes place. The Elastic Recoil Detection Analysis (ERDA) provides excellent tools for the on-line characterization of samples and depth profiling.

Nuclear Regime

For ion energies exceeding the Coulomb barrier there are inelastic collisions giving rise to nuclear reactions providing unlimited possibilities with Nuclear Reaction Analysis (NRA) techniques for specific nuclei connected problems. Nuclear reactions can be tailored to generate trace quantities of radioisotopes inside the material. This provides the method of Thin Layer Activation (TLA) analysis for accurate on-line measurement of wear with sensitivity ranging from atomic layers to micrometers.

3 Passage of SHI in Materials

Swift Heavy Ion (SHI) penetrating matter interacts through Coulomb forces mainly with the target electrons. It can give a sharp impulse to an electron as it swiftly passes by. The energy transferred to the electrons through inelastic collisions is the energy loss of SHI which essentially makes it slow down. The target atoms are excited and ionized through these collisions. The energy transferrred to the positive ion created by ionization is, in general, negligible. Further, encounter between SHI and nucleus to produce nuclear reaction or scattering is negligible and does not contribute to slowing down process. The energy loss dE/dX, basically has three contributions.

$$dE/dx = (dE/dX)_{\text{electronic}} + (dE/dX)_{\text{nuclear}} + (dE/dX)_{\text{radiation}}$$

The energy loss in radiative processes - such as bremsstrahlung and Cerenkov radiation for heavy ions is very small and can be neglected in our discussion. The most important energy loss mechanism, particularly at high energies, is the interaction of the effective charge with the target electrons. The nuclear energy loss dominates at very small energies ($E \leq 10$ keV/u) which is caused by the scattering of the projectile at the screened nuclear potential of the target atoms (Rutherford Scattering). Because the recoil energy transferred to target atom is frequently higher than the binding energy, these atoms are released from their chemical environment and can trigger off a chain reaction if kinetic energy is big enough. However, the dominance of the nuclear collision process is restricted to very low energies. Fig. 1 shows the nuclear energy loss, also called nuclear stopping power S_n, for two

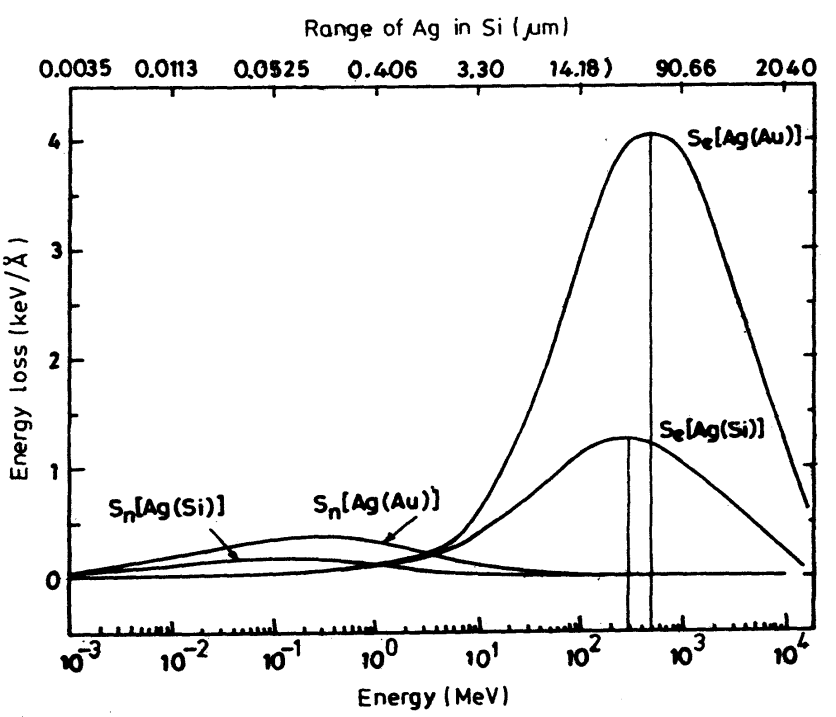

Fig. 1 The energy loss, nuclear and electronic of Ag ions in Si and Au targets over an energy region upto 10 GeV. The figure also shows the range of Ag ions in Si for the energies on X-scale.

cases, Si and Au targets with Ag beam, with peaks around 5 keV/u.

Electronic Energy Loss

For energies greater than 10 keV/u the electronic stopping power S_e dominates the stopping process described by the Bethe-Bloch equation.

$$S_e = \frac{dE}{dX}\Big|_e = \frac{4\pi e^4 Z_{eff}^2 NZ}{m_e v^2} \quad \ln \frac{mv^2}{I_o} + \text{relativistic terms}$$

where Z_{eff} is the effective charge of the projectile, Z the atomic number of the target atoms, v the projectile velocity, N the density of target and I_o mean ionization potential. The stopping powers are tabulated by Northcliffe and Schilling[1]. For light ions like He the maximum of S_e is at ~0.15 MeV/u and has a value of 0.2 keV/Å. Fig. 1 also shows values of S_e along with S_n for Ag ion beam for energies over a wide range upto 10 BeV for penetration in two targets Si and Au. The electronic energy loss peaks at 2 to 4 MeV/u with a value varying from 1 keV/Å for silicon to 4 keV/Å for Au target. Fig. 2 shows S_e for three different ion beams O, Ni and Au on gold target. The energy loss peaks at widely varying energies and decreases at higher energies allowing wide variation of S_e by appropriate choice of projectile. The figure also shows the range of Oxygen ions in Au, which makes it clear that the maximum S_e achievable with these ions in Au is 10 MeV having range of 2.7μm.

In the region where the electronic energy loss predominates, the energy lost from the primary ions is mostly transferred to the electrons. Depending on the initial energy, 65-70% of the energy loss is transferred into the kinetic energy of the electrons, 15-25% of the energy is used up to overcome the binding energy and only 5-15% is consumed for electronic excitations. Thus most of the electrons are liberated from their atomic binding.

So, the ion loses energy by two independent means: elastic collisions with the nuclei of the target giving nuclear stopping power S_n (nuclear energy loss) and inelastic collisions with electrons of the materials S_e (electronic energy loss).

$$S(E) = S_e(E) + S_n(E)$$

The energy loss is also referred as Linear Energy Loss (LEL), particularly in radiobiology. Fig. 3 shows variation of energy loss of 270 MeV silver ions due to

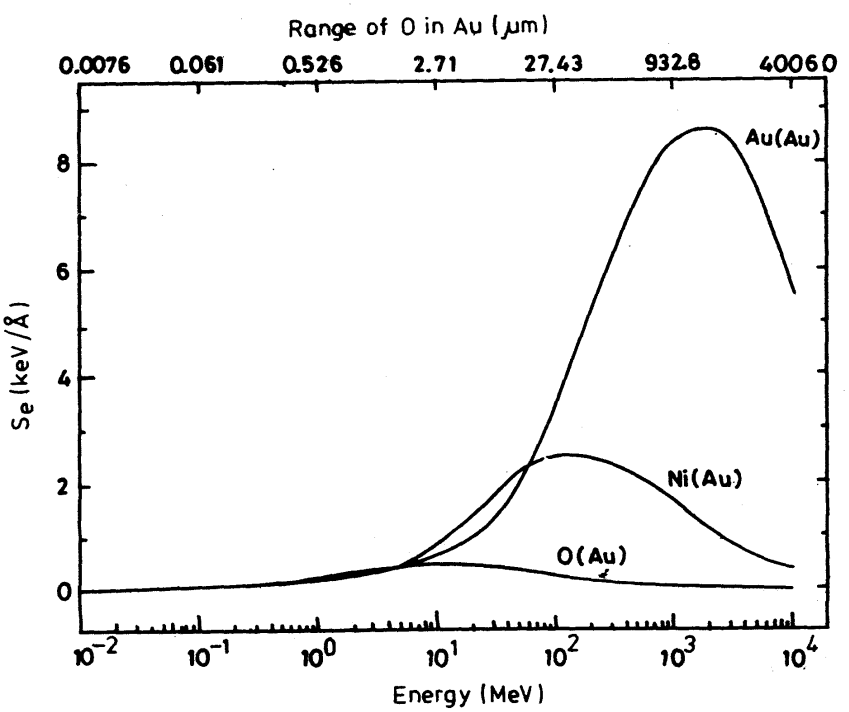

Fig. 2 Electronic energy loss in Au of O, Ni and Au over a wide energy interval

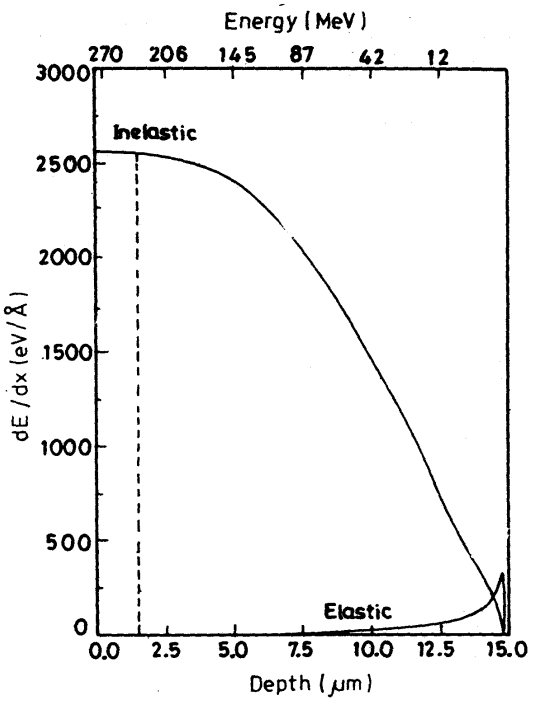

Fig. 3 Variation of the energy loss of 270 MeV silver beam due to inelastic and elastic collisions *versus* the depth from the surface of YBCO. The corresponding energies at various depths are mentioned

inelastic and elastic collisions *versus* the depth from the surface in a YBCO target. The corresponding energies at various depths are listed on top of the figure as X-scale. It illustrates that as the ion penetrates it loses energy depositing it in electronic system (inelastic scattering) with linear energy transfer at the rate of S_e ~ 2.6 keV/A. S_e remains constant upto a depth of ~1μm and then gradually reduces. The nuclear energy loss S_n is negligibly small till the fag end of the range.

SHI Induced Damage

Normally when we speak of radiation damage we have in mind cascade of atomic collisions leading to the formation of defects - predominantly Frenkel pairs and embedment of projectile ion in the material towards the end of its range.

The characteristic of SHI is to deposit most of its energy (S_e) on the target electrons, which can be excited or ionized. De-excitation of atoms results in photons. In the ionization process the released electrons which leave their parent atoms have a broad spectrum of kinetic energies. These electrons can have energies upto several keV, and therefore can trigger some ionization of their own. Thus many of them will knock out secondary electrons resulting in multiplication. This electronic collision cascade, called δ electrons, spreads out rapidly and carries away energy and charge from the ion trajectory. A core of positive target ions remains. The delta rays have ranges which are very small compared with the range of SHI. Thus, it is immaterial whether the energy is deposited in the material directly by the primary particle itself or by secondary delta rays. This energy deposited in electrons can be coupled into atomic mode of motion, the mechanism of which is not well understood in most cases. The damage created by this electronic stopping power (S_e) or Linear Energy Transfer (LET) depends on the physical properties of the material. SHI induces amorphization in many crystalline insulators. The amorphous phase along the ion trajectory can form continuous track at appropriate values of S_e

Dengler *et al.*[2] showed that in yttrium iron garnet continuous tracks are formed only at S_e greater than a threshold value. Houpert *et al.*[3,4] have shown that in $Y_3Fe_5O_{12}$ spherical defects of 1.5 nm radii appear for $4.5<S_e<7$ keV/nm, which become elongated defects for $7<S_e<14$ keV/nm and for higher S_e values tend to become more and more cylindrical with increasing radius. The defects take shape of long homogeneous cylinder for $S_e > 20$ keV/nm.

Latent Track

The continuous track of defects forming a cylindrical modified zone of material in the wake of a single SHI is called a latent track or columnar defect. It was believed that latent tracks are formed in insulators (silicates, oxides, plastics, glasses etc.) but not in good electrical conductors (metals such as Ag, Al, Cu etc.) and semiconductors such as Si and Ge. It is now believed that above certain threshold values of S_e almost all materials can get modified in columnar region and possibly form tracks.

Struder *et al.*[5] have studied the track formation in relation to amorphizability of materials. Pure metals which are amorphizable by conventional methods do not give rise to latent tracks but their sensitivity to S_e is seen as discontinuous tracks. In amorphizable alloys

such as $NiZr_2$ tracks exhibiting an amorphous core have been observed.

In metallic targets, track formation is much more difficult which is understood as owing to the presence of numerous mobile electrons spreading fast the deposited energy. With the availability of swifter heavier ions, structural columnar shaped changes have also been observed in many metallic systems[6-8]. High S_e effects in amorphous materials display[9] macroscopic deformation of ~10% above an incubation fluence in the form of anisotropic growth. The sample shrinks along the beam direction and expands in the two perpendicular directions.

Columnar defects have not been observed in semiconductors (Si, Ge) even with the highest S_e available (GeV U ions). It is surprising since these materials are amorphizable by conventional techniques. On the other hand, for semiconducting compounds such as GeS which are easily amorphizable, one finds tracks with amorphous core. Interestingly in amorphous silicon or germanium layers, tracks have been observed due to cylinders of recrystallized matter. It is observed[5] that iono-covalent materials such as Al_2O_3 and magnetic Fe_3O_4 can be damaged in the form of discontinuous non amorphous tracks. On the other hand all amorphizable iono-covalent materials exhibit amorphous tracks with variable sensitivity.

Physics of the Track

The tracks are localized regions of modified material created by a process other than by direct displacement of lattice atoms by the projectile ion, which occurs at low energies. How this modification occurs requires understanding of the physical processes involved. The path of SHI is strewn with free electrons and positively charged ions (atoms of the target of interest with missing electrons). There are thousands of such electron ion pairs formed directly by SHI and then as pointed out earlier, there is cascade of delta electrons. The energy loss by the slowing down of SHI is shared between electrons by electron-electron interaction and is then transferred to lattice atoms by electron-phonon coupling. A core of unbalanced holes results since the energy transfer to electron ejects them from the path of the ion. The problem in describing the track is to understand the evolution of the electrons, holes and excitation with time after the primary excitation events. In a metal the ionizations are screened very quickly by the free electrons (within 10^{-15} seconds), whereas the ion core in a insulator may survive for much longer times ($<10^{-11}$ seconds). The cylindrical region with the ionized atoms experiences Coulomb repulsion between the holes. If this situation remains for sufficient duration, it can create movement of lattice atoms from their sites. This is referred to as Coulomb explosion situation which can result in the damage of the material.

The situation can also be viewed from the view point of the temperature inside the columnar region, which can be high enough to melt the material. The electrons around the ion trajectory are highly excited and fraction of this energy is transferred to the host atoms close to the trajectory. The numerical solution of heat flow equations shows[10] that this energy may be sufficient to raise the lattice temperature well above the melting point. In insulators, the temperature increase is confined in a small cylinder and may last for $\sim 10^{-12}$ sec depending upon the diameter of the cylinder and diffusivity of the target. The process results in the formation of an amorphous phase. It is clear that the physical process inside the cylindrical region will depend upon many parameters: electronic energy density, how fast the ionized atoms get back their electrons, conductivity of the target, electron-phonon interaction etc. The highly repulsive electrostatic forces which act during the period before target atoms get neutralized can give rise to explosion within 10^{-15} sec and, besides local damage (track), produce shock waves. In the so called thermal spike model, the latent track can result from the rapid quenching of the entire cylinder of the molten matter.

4 Surfaces, Interfaces and Multilayers

Ion Beam Induced Adhesion and Stitching

The performance of tribological coatings depend greatly on the adhesion of film on substrates. In most situations a bond is required between the two materials having little chemical affinity for each other, which has to withstand abrasion and peeling, and should be able to survive thermal cycling. Some of these requirements are sometimes contradictory. Ion beam interactions can produce dramatic changes in the mechanical properties

of thin films on various types of substrates. Low energy ion implantation through the interface improves adhesion, but the ion range limits the acceptable thickness of the initial film. The doses employed are high (upward of 10^{16} cm^{-2}). Modification is due to the creation of elastic collision produced damages and chemical effects. The energy loss in inelastic processes is very high for SHI which can produce complex changes in the film, the interface and/or the substrate. The possible implications of this energy loss for interface stitching has been explored relatively recently. There is an indication that both ionizing (S_e) and ballistic nuclear collisions serve to disorder the interface structure.

Modification of chromium coating by 75 MeV nickel ion beams has been studied[11] under the condition that the range of the ions is many times the film thickness (1μ). This ensures that the end of the range effects where energy loss is predominantly nuclear are placed deep inside the substrate rather than near the interface. The electronic energy loss in the coating was fairly uniform in depth with the value of 1.8 keV/Å, and was over two orders of magnitude higher than the nuclear energy loss. The coating hardness was observed to increase significantly even at moderate doses with ions having range many times the film thickness.

Sputtered TiN coatings on stainless steel were irradiated with 210 MeV Ag ions and studied[12], before and after irradiation to dose of 8.6 x 10^{14} ions cm^{-2}, using scratch adhesion tests. Significant improvement in tribological properties, indicated by the average load at which various scratch induced failure modes commence for TiN coating on SS, was observed in irradiated films. Ag ions at 210 MeV deposit electronic energy at the rate of about 2.6 keV/Å in TiN film, whereas the average nuclear energy loss at this energy is only 7 eV/Å. Clearly, fast moving ions can produce complex changes resulting in an improvement in the adhesion. An experiment[13] with a few micron thick MoS_2 film on stainless steel substrate using SHI indicated significant improvement in the adhesion without any deterioration in the frictional property. Irradiation also improved the load bearing capacity of the coating. The improvements in tribological properties with high energy irradiation are comparable[14] to those possible with low energy ions. Besides the advantage that thicker films can be treated, it is found that dose required for high energy ions is several orders of magnitude smaller.

Ion Beam Mixing

Ion beam mixing is an ideal way of making films of compounds such as nitrides, carbides etc. The mixing is achieved by irradiation with keV energy ions which utilizes the kinetic energy of ion beams to mix predeposited surface layers with substrate materials. The limitation at low energy due to small ranges of ion has been overcome by combining ion-beam mixing with simultaneous deposition. Use of heavy ions give high mixing efficiencies which is attributed to enhanced mass transport during the cooling phase of energetic displacement cascades, i.e. radiation enhanced diffusion. The role of electronic excitation in mixing is now being investigated.

Intermixing at the interface using swift heavy ion irradiation has been studied[15] in a number of multilayers e.g. Ni/C, Pt/C, Fe/Si with Ag ions in the energy range 100 to 200 MeV. The irradiation induced effects were studied using X-ray reflectivity and X-ray diffraction measurements. The modifications were observed in all the three multilayers at $(dE/dX)_e$ values which are much below the predicted threshold values of damage production for the corresponding metal species. This effect is attributed to the small thickness and/or discontinuous nature of the metal layers. It has been suggested that decreased mobility of the conduction electrons due to interface scattering may result in the confinement of the deposited energy to a smaller region thus raising its temperature to sufficienty high value for interdiffusion to occur. Strong intermixing has been observed in the case of Ni/C and Fe/Si multilayers, while in case of Pt/C multilayers, under similar irradiation conditions no significant intermixing has been observed. These results suggest that chemically guided defect motion also plays a significant role in the mixing process associated with swift heavy ion irradiation. In case of Fe/Si multilayers, the effects of irradiation were very different from those of thermal annealing.

Irradiation Effects in Magnetic Multilayers

Effect of swift heavy ion irradiation on the magnetic and magnetotransport properties of Fe/Tb and Fe/Cr

multilayers have been studied[16]. In the case of Fe/Tb multilayers, irradiation with 80 MeV Si ions caused the ion perpendicular magnetic anisotropy (as measured by Mössbauer spectroscopy) to decrease with irradiation. Combined results of X-ray reflectivity and Mössbauer measurements suggest that irradiation caused interface roughness to increase without introducing any intermixing. Possible effects of irradiation also include stress relaxation in the films. Irradiation with 150 MeV Ag ions resulted in intermixing at the interfaces accompanied by a large decrease in perpendicular magnetic antisotropy.

Atomic mixing induced in metallic bilayers of Ni/Ti irradiated at 80K with ions of Pb, Ta and U showed[17] a very strong mixing. The observed mixing efficiency was observed to be two orders of magnitude higher than that induced by elastic collisions.

Electronic Sputtering

An ion beam striking a surface produces sputtering. The yield, average number of target atoms ejected per incident ion, is about unity for low energy (keV) ion beams where the ion velocity is ~4×10^7 cm/sec which is small compared to the smallest velocity of orbital electron (2×10^8 cm/sec). The sputtering in this energy region is due to the cascade of collisions, and the ejection is a result of direct momentum transfer from ion to atom of the solid. At higher energy (MeV) where ion velocity is ~10^9 cm/sec, the energy transfer through ionization is the principal mode of energy loss. The leads to ejection of surface species which is known as electronic sputtering. The sputtering yield increases significantly with the electronic energy loss, S_e. Large number of molecules are ejected by a single ion. Buckyballs and other fullerenes have been observed[18] from the heavy ion tracks in polymer $(C_2H_2F_2)_n$. An individual SHI produces high excitation density in a cylindrical area of the order of a few square nanometers in ~10^{-14} sec. In this cylindrical volume it appears that the molecules are ejected intact from the surface, although inside the track they may be destroyed. It is observed that large numbers of both small and large molecules can be ejected by a single SHI and that the yields depend on S_e. High excitation densities can also be achieved using laser pulses over areas of the order of square millimeteres where it takes ~10^{-8} sec to get the high excitation density at the surface giving rise to ablation. In the case of SHI, a hot core of a few square nanometers is produced in less than 10^{-14} sec. It is believed that the very rapid excitation and ejection can produce gas phase biomolecules with low enough levels of internal excitation so that the molecules as heavy as about 40,000u can remain intact until detection. This ejection induced by SHI offers immense possibilities for mass spectrometric studies of macro-molecules and has been studied by Upsalla group[19-20]. It is concluded that the sputtered species yield varies with excitation density and on the size of the ejected ion. It is suggested that intact ions are ejected due to shock wave emanating from the columnar track region produced by SHI. Both ionized and neutral intact leucine molecules were observed in the sputtered material. The observations and molecular dynamics based analysis has led to some understanding of the process of electronic sputtering[21]. SHI can eject an intact bovine insulin molecule ($C_{254}H_{377}N_{65}O_{75}S_6$) from a solid sample of bovine insulin and eject a "buckyball" (C_{60}) from $(C_2H_2F_2)_n$. Molecules are formed in the highly ionized region of inner radius of about 0.4 nm. Large intact ions are ejected from region between 0.4 nm to 2nm, large intact neutrals from region between 2 to 4 nm and at larger distances transported thermal energy and the tail of secondary electron distribution act to modify the material, cross-linking of molecules in organic materials[22].

Study of the surface morphology of SHI irradiated materials is of considerable interest as it can provide some clues to the interaction of ions with the atoms on and near the surface. Thibaudau *et al.*[23] studied mica irradiated with GeV energy Kr ions with an AFM. *In situ* STM study of surfaces are now being planned with NSC Pelletron for SHI irradiated surfaces with varying S_e values to examine the changes on atomic level which occur at the surfaces.

5 Semiconductors and Devices

Heavy ion beams allow unique opportunities for the modification of the electronic properties of materials and to form novel device structures. Swift heavy ion implantation has potential applications especially for the formation of buried conducting or insulating layers. However, radiation induced defects in this energy range need to be investigated. SHI interacts with the lattice

through the electronic process during most of its range except near the end where it is implanted at predetermined region. Although the heaviest damage occurs in the region where the ions stop, there is some damage at shallower depths which needs to be studied for proper exploitation of these in tailoring the material. In semiconductors, silicon is found to be very insensitive to electronic loss. As mentioned earlier, even the GeV uranium ions do not produce ion tracks. The fact that the loss of energy to the target material is by electronic interactions without direct impact with atoms is exploited to produce modifications that are very different from those obtained through keV ion bombardment.

Structural Changes Induced by SHI

It is important to study the extent of lattice deformation in spatially separated electronic and nuclear energy loss regions. This has been studied[24] in Si(100) crystal with 100 MeV Ti ions using X-ray topographic techniques. Controlled surface etching and subsequent topography is performed to extract information about the distribution of the strain in the depth of the crystal. Si(100) single crystal, 500μm thick, was irradiated with 100 MeV Ti ions (dose~ 10^{12}. ions cm^{-2} through a metal grid providing 0.8 x 0.8 mm^2 openings separated by 0.04 mm. The range of 100 MeV Ti in Si is 20μm. Topographs with various diffraction vectors were recorded using Mo and Cu K-alpha X-rays to cover: (i) total range of impinging ions (up to 22μm), (ii) shallow surface region (~7.5μm) well separated from the elastic loss region and (iii) up to 27μm to investigate the elastic loss region and beyond in the interior of the sample.

It was observed that only the masked regions are under strain whereas the irradiated region near the surface (7.5 μm) does not show any strain. In the elastic loss region (~ 22 μm) strain is observed along the normal to the surface, in contrast to the in-plane strain at the boundaries. Masked regions are observed to be under compressive stress. The compressive nature of the strain along the grid is consistent with the assumption that the irradiated surface regions possess tensile stress which accumulates at the surface discontinuation defined by the grid. Depth distribution obtained up to 8 μm by etching in several steps indicated that the in-plane strain field is not a surface feature but penetrates substantially deep below the surface. It is concluded that the masked regions are under compressive strain parallel to the sample surface. It indicates a tensile stress generation in the electronic loss region. The stress is concentrated at the boundaries. The implanted region experiences out-of-plane (along the surface normal) strain.

Defect Profiles

Structural changes have been investigated[25] with much higher energy and heavier ions. It was observed that the lattice constant increased by 1.4 x 10^{-4} nm in the case of 42 Me V/u, Kr ions (dose 1.9 x 10^{12} ions/cm^2). Fine structural changes, increases of lattice parameter by 1 x 10^{-4} Å, in the near surface layers are observed with 4 MeV/u neon ions, but not with 4 MeV/u oxygen ions[26].

High Energy Implantation

Transport properties of high energy (70 MeV) ^{120}Sn implanted on GaAs and the effect of annealing on the electrical properties of the implanted layer has been studied[27]. The damage profile of the GaAs substrate implanted to a dose of ~10^{14} ions/cm^2 was studied by etching the samples to different depths by a suitable chemical etching. The resistance and optical density measurements showed that the disordered regions are of three types. There is a damaged surface region followed by a large region with negligible damage and highly disordered region near the end of the ion range. The surface modification/damage resulting from electronic energy loss is restricted to narrow region. Most of the material seems to be unaffected except the implantation zone. There is also evidence of some annealing of inherent defects in the material due to S_e, depending on its values.

An experiment[28] was done to see how the impurity concentration changes with depth due to electronic energy loss. Samples of *n*-type crystalline silicon were exposed to different fluences, ranging from 1.25 to 5x10^{14} ions cm^{-2}, of 90 MeV silicon ions. The induced disorder in the surface region was studied by grazing angle X-ray diffraction and optical reflection spectroscopy, and that in the bulk was studied by measuring the life-time of the excess minority carriers generated by a 1 MeV pulsed electron beam. Both in the surface region as well as in the bulk, the degree of

induced lattice defects was found[28] to increase with increase in the ion fluence. These results indicate that 90 MeV silicon ions create an appreciable number of defects in crystalline silicon, the concentration of which increases from the surface to their projected range of 21μm, and at higher fluences, secondary defects are also produced in the bulk. Even at the highest fluence used, the energy deposited through electronic loss had no observable effect on the annealing of the induced defects.

In crystalline silicon, irradiated with 60 and 80 MeV energy silicon ions, regions of high defect densities were located by repeatedly etching the sample and measuring the lifetime of minority carriers, τ. The values before etching were 10 and 8μs in the 60 and 80 MeV ion irradiated sides respectively, and 19μs in the unirradiated side. On etching the samples, these values of the irradiated side initially increased steeply. However, the value of τ in the unirradiated side remained unchanged even after etching. These results show that the regions of high defect densities are situated below the surface at depths of 20 and 27μm respectively, in 60 and 80 MeV ion irradiated samples. These coincide, respectively, with the projectile depth in silicon at which the 60 and 80 MeV silicon ions deposit a maximum amount of energy through nuclear collisions[29].

On-line resistivity measurements[30] of samples as a function of fluence indicate that the resistance first decreases on irradiation up to a certain dose in the range of 10^{11} to 10^{13} ions/cm^2, beyond which it starts to increase. One such measurement was done on thin GaAs crystals with 100 MeV Si ions. It may be mentioned that the maximum S_e possible with Si beam in GaAs is ~0.5 keV/Å which occurs at 30 MeV beyond which it decreases. 100 MeV ions were used to keep S_e~0.4 keV/Å throughout the thickness of the GaAs film. The decrease in resistance can be understood in terms of reduction of defects caused by the annealing due to electronic energy dissipated in the film. As the fluence increases, the defect creation seems to overtake the annealing process.

Amorphous chalcogenide semiconductor $Pb_{20}Ge_{19}Se_{61}$ was irradiated with 75 MeV Ni beam with a fluence of 5 x10^{13} ions/cm^2. Measurement of electrical conductivity and thermoelectric power indicated[31-32] that the Ni atoms with 3d electronic shell induce deep trap state near the Fermi level which contribute to the electronic conduction process. The carrier transport remained p-type after irradiation and annealing. It is interesting to note that 75 MeV Ni at a fluence of 5 x 10^{13} ions/cm^2 produce significant doping effects in chalcogenide glass.

Photoluminescence properties of SHI irradiated porous silicon has been investigated. An order of magnitude increase in the efficiency in photoluminescence was observed in silicon and phosphorous ion irradiated porous silicon[33].

Surface Roughening Induced by S_e

Spectacular increase in surface roughness of Si (111) surface due to 200 MeV Ag ion irradiation at a fluence of 5x10^{13} ions/cm^2 has been observed[34]. It is ascribed to the displacement of Si atoms driven by the creation of unsaturated dangling bonds created by SHI. The Si surface shows a dramatic surface modification even beyond the fluence when the total surface gets covered with damaged zones at critical fluence of 10^{12} ions/cm^2, a situation quite different from that observed in metals and insulators[35].

Tailoring of Switching Times of Silicon Diodes

Radiations can improve the switching characteristics of diodes but the defects increase the forward voltage drop (V_f). SHI can be used effectively to control the switching parameters without affecting the forward voltage drop very significantly. The switching time of silicon diodes decreased from 1000 ns to 50 ns by introducing ion induced defects into the n-region of silicon junction diodes. These diodes were made on 250μm thick silicon wafers without adopting a gold diffusion process. The junction was located at a distance of around 180mm from the surface of the n-region. The switching characteristics of the diodes are controlled mainly by the charge carriers of the n-region. The life time of minority carriers in the n-region has been reduced by inducing defects through heavy ion irradiation. The diodes were irradiated with 100 MeV silicon, 70 and 80 MeV oxygen, 65 MeV boron and 35 MeV lithium ions. In this way, defects could be induced at different locations in the n-side covering a range from 35μm to 170μm away from the contact of the n-side. It has been observed that the defects produced near the junction are more effective in reducing the turn-off time, τ, as compared to those produced near

the surface. On comparing the values of τ, for different diodes, it has been found that the defects induced by 65 MeV boron and 35 MeV lithium ions are most effective because even for a large decrement of τ, the corresponding increment in the V_f was less than 0.2 V. For other ions, though the decrease in τ was effective, it was followed by a large increment in the V_f. In all the ion irradiated diodes, the increase in the V_f could be recovered partially after annealing the diodes at 450°C. Results indicate that heavy ions can be used effectively to control the switching parameters of diode[36].

6 Oxides: HTSC and CMR

High Temperature Superconductors

A limit on technological applications of high temperature superconductors (HTSC) comes from the intrinsically low critical current density J_c and from the ease with which magnetic vortices can move. All HTSC are type II superconductors and beyond a certain value the applied magnetic field penetrates in the form of flux lines, each carrying an elementary flux quantum. If current is passed, Lorentz force moves these flux lines which generates an electric field leading to dissipation. This limits the critical current densities in HTSC materials. Due to their well defined cylindrical shape, columnar tracks provide efficient pinning centres. Every SHI, if its electronic energy loss S_e exceeds a material dependent threshold S_{th} (typically of the order of 1.2 keV/Å for HTSC), creates one latent track of disordered material in the HTSC along its path. Such a columnar defect is very similar to the shape of a flux line and thus tailors defects for vortex pinning which improves J_c by an order of magnitude. The pinning is most effective when the defects are continuous and applied magnetic field is parallel to the axis of the columns. The optimum result is expected when the diameter of the continuous columnar defects is of the order of the coherence length.

Introduction of columnar defects is expected to improve the properties of cuprate superconductors for device applications. For the fabrication of superconducting microwave devices such as circulators and Faraday isolators, where the films are subject to magnetic fields, it is essential to be able to control dissipation due to the motion of vortices. This can be done by locking the vortices to the columnar defects.

Microwave absorption in YBCO thin films with columnar defects was studied[37] by measuring the angular dependence of microwave magneto absorption of both pristine and 270 MeV Ag ion irradiated YBCO c-axis oriented films (~1800 Å thick on $LaAlO_3$ substrates). The fluence varied between 0.5 and 8.0 x 10^{11} cm^{-2} and the columnar defects were aligned 5°±1° away from *c*-axis to avoid ion channeling. The microwave absorption was studied by placing the sample in an alpha cavity operating at ~10 GHz and studying the temperature and field dependence ($0 \le B \le 1.5$ T) of $P_c(B, T)$ the power reflected at cavity frequency. For the field induced absorption the sample was zero-field cooled to the temperature of interest and the field slowly ramped to ~ 1.5 T. The angular dependence of $\Delta P(B, T, \theta) = [P_c(B, T, \theta) - P_c(B=0, T)]$, where θ is the field tilt with respect to the sample ab plane, was studied by rotating B from the ab plane to the *c*-axis with b_{rf} normal to B at all angles. The introduction of columnar defects has several consequences. The most telling result of the present investigation is the difference between the angular dependence of $\Delta P(B, T, \theta)$ seen in the pristine and its irradiated counterpart (Fig. 4). Pristine sample shows a simple ($C_1 + C_2 \sin \theta$) variation but the irradiated sample shows a marked dip at $\theta = \pi/2$ where B is aligned parallel to the columnar defects. The dip was observed to increase with the fluence. Data at

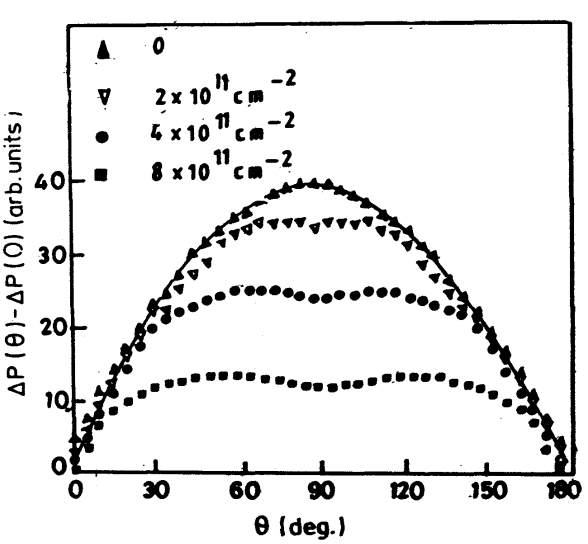

Fig. 4 The angular dependence of microwave magnetoabsorption of YBCO films at various fluence at 1.2T, 77K and 10 GHz.

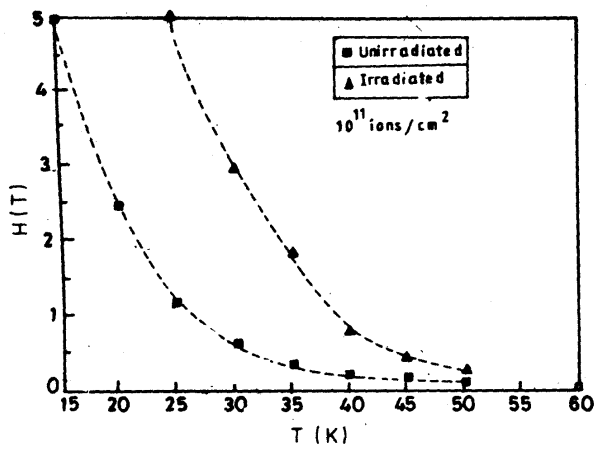

Fig. 5 The shift of the irreversibility line (IL) towards higher temperatures after irradiation (at a fluence of 10^{11} cm^{-2}) of the single crystal of BSCCO

higher fluence exposure is required to determine the optimum fluence.

However, even with this fluence, microwave loss in sample at 77 K and 0.5 T was reduced by a factor of more than two as compared to that of pristine sample. Fig. 5 shows the magnetically determined irreversibility lines of as grown and irradiated single crystals of BSCCO. The shift to higher temperature after irradiation crystals is clear[37]. The increased pinning by columnar defects was clearly evident at 10 GHz but increasing the frequency to 32 GHz indicated that columns are very effective in pinning[38].

Far-infrared transmission of YBCO films with columnar defects was measured[39] from 20 to 150 cm^{-1} at 6K in the magnetic fields of 0--9T. Irradiation with 270 MeV Ag ions increases the zero-field transmission, but the change in transmission with applied field is observed to be independent of defect density. The change in transmission produced by irradiation can be understood by imagining columnar defects as normal metal in superconducting background.

The double peak low field anomaly in the magnetization hysterisis loop in BSCCO single crystals was observed[40] to disappear with columnar defects produced with 200 MeV Ag ions and fluences varying from 10^{11} to 10^{12} ions/cm^2. It is ascribed to the partial destruction and ineffectiveness of dislocation networks in the CuO_2 planes of the BSCCO crystal. The observed shift of irreversibility line to higher temperature predicts that, not only is flux pinning the origin of this line but also columnar defects enhance flux pinning with an increase in the 3D to 2D crossover temperature in these crystals.

Influence of columnar defects produced by 250 MeV Ag ions on magnetotransport and magnetization properties of BSSCO was studied[41]. It was shown that there is significant reduction of the long tails in magnetoresistance curve and narrowing of the transition in ac susceptibility in high fields due to the enhanced correlation between superconducting layer by columnar tracks.

Modifications in HTSC with S_e Below Threshold Value

Modifications in the properties of cuprate superconductors with SHI depend crucially on the value of S_e. Large number of studies using ion beams giving $S_e > S_{th}$ have led to a good understanding of application of columnar defects, as discussed. The situation, however, is more complex when ions produce $S_e < S_{th}$. Effects produced depend on the pre-irradiation defect structure of the material, e.g. local stoichiometry, point defects present, twin and grain boundaries etc. SHI irradiation of cuprates has been shown to induce varied effects like increase in the normal state resistance, a progressive metal to insulator transition and normally lowering of their superconducting transition temperature (T_c). An *in situ* measurement on Bi-Pb-Sr- Ca-Cu-O (BPSCCO) bulk superconductor with 100 MeV oxygen ion irradiation showed[42] a decrease in resistance without change in T_c at fluence of less than 3.0 x10^{12} ions cm^{-2}. However, the irradiation caused lowering of the zero resistance temperature and increase in the room temperature resistance at fluence exceeding 3.0 x 10^{12} ions cm^{-2}. It is shown that the presence of grain boundaries play a major role in these phenomena, which are due to mobile irradiation induced defects. Resistance variations for specimens depend upon the relative proportions of the phases $Bi_2Sr_2Ca_1Cu_2O_{8+y}$ (2212) and $Bi_2Sr_2Ca_2Cu_3O_{8+y}$ (2223). However, in this experiment no indication of formation/increase of 2223 phase was evident in XRD pattern and so the lowering of resistance could not be correlated with the increased proportion of the 2223 phase. Although the sample exhibited decreased resistance and increased J_c, it did not show significant changes in T_c. At higher fluence, exceeding

3.0 x10^{12} ions cm^{-2}, resistance increased with fluence accompanied by a decrease of J_c and a decrease of T_c by 7 K. The ion-induced effects are associated with the displacement of the intercalated excess oxygen atoms. The films with better superconducting properties i.e. lower R and higher T_c, do not show the decrease in resistance with fluence.

Phase transformation (2212) → (2223) was observed[43] in a mixed phase Bi based oxide superconductor when irradiated at 80 K with 100 MeV Fe ions. The sample contained 40% of (2223) and the rest was made up of (2212) phases. In an earlier experiment at room temperature no phase transformation was observed, but an increase in the normal state resistivity was observed[44].

Granularity Controlled Irradiation Response of Cuprate Superconductors

Understanding the radiation response of high T_c superconductors is important for predicting the radiation survivability of the devices made from these materials (i.e. SQUIDs, sensors, delay lines etc.) operating in natural or hostile radiation environments. Cuprate superconductors exhibit a great sensitivity to irradiation induced defects. The sensitivity of $La_{1.8}Sr_{0.2}CuO_4$ is a factor of 2 higher than that of $YB_2Cu_3O_{7-x}$ which in turn is about a factor 2 more sensitive than the chevrel phases and a factor of 20 to 40 more sensitive than A15 superconductors. The high sensitivity of oxide superconductors to ion irradiation is believed to arise due to their lower density of states at the Fermi level and their particular structure where oxygen content and disordering are easily affected. Further, the cuprate superconductors are granular in nature. It is known that the response of such a medium to ion irradiation can be very different from that of a single crystal. This is particularly true when the dimension of the spatial inhomogeneity approaches the area/volume of the irradiation induced disturbed zone. In this case, the finite volume of the grains imposes constraints on the dissipation of the energy deposited by the ion beam. Further, in granular HTSCs, the damage efficiency of the high energy heavy ion beam, interacting predominantly through electronic energy loss mechanism is widely different in conducting grains as compared to that in insulating grain boundaries. Thus, in low fluence regime where amorphization is prevented, the response of the cuprate to ion irradiation has been shown to be strongly influenced by their grain boundary characteristics.

To improve the radiation resistance of the cuprate superconductors so that the devices made out of them can be used in radiation environment, it is therefore necessary to make both the grain and the grain boundary insensitive to ion irradiation. In a set of $YBa_2Cu_3O_{7-x}$ (YBCO)/Ag composite thick and thin films, it is seen[45] that Ag present either at the grain boundary or in the grains suppresses the sensitivity of the composite system to ion irradiation. Thus, the superconducting transition/ width and normal state resistivity in YBCO/Ag (5wt%) composite thin films were found to practically remain unchanged up to a fluence level of $8x10^{14}$ ions/cm^2 under irradiation with 140 MeV Si ion at 78 K[45]. The role of Ag substituting chain Cu ions in the grains and thus inducing radiation resistance to the films has been analyzed through a crystallochemical approach[46]. According to this approach, Ag with its two-fold oxygen coordination locks two nearby oxygen vacancies and reduces the mobility of the chain oxygens under irradiation. Remaining at the grain boundaries, Ag brings about considerable microstructural modifications converting most of the s-i-s type junctions to s-n-s type. The defect creation mechanism through electronic energy loss of the high energy heavy ions is therefore suppressed. Suppression of irradiation response in YBCO/Ag thick films when irradiated by 250 MeV Ag ions which have an electronic energy loss greater than that required to create amorphised latent tracks in YBCO medium is also seen.

Granularity in high T_c cuprate superconductors has remained as one of the complex problems due to their shorter coherence length, high superconducting anisotropy and reduced dimensionality. The response of these systems to SHI irradiation in particular is complex due to higher sensitivity of the grain boundaries to irradiation induced defects as compared to that of the grains. Extraction of granularity parameters like the weak link resistivity, paracoherent resistivity and percolation factor from the temperature and current dependent resistivity in the normal and superconducting state based on granularity controlled current percolation model, and the variation of these parameters with ion fluence has enabled[47] us to isolate the intra - and inter-granular response of YBCO to ion irradiation and study

the evolution of these parameters with ion fluence[48]. Irradiation with lighter ions like 120 MeV S which does not create amorphized latent tracks ($S_e<S_{th}$) is seen to cause grain alignment in sintered YBCO thick films as revealed from the enhancement of current percolation factor with ion fluence.

Transient Behaviour During Irradiation

A study of transient behaviour of resistivity during irradiation of films has been carried out[49] with an aim to understand the mechanism of creation and annealing of defects in cuprate superconductors. Thin films (~3000Å) of YBCO deposited on $LaAlO_3$ were irradiated with 100 MeV O ions at room temperature and at 100°K with ~2.0×10^{10} ions cm^{-2} sec^{-1} for a few seconds and resistivity measured continuously during the irradiation and after turning the beam off. The resistance increased by a few per cent (Fig. 6) with this fluence and quickly relaxed to pre-irradiation value. For thick films opposite behaviour was observed during the beam-on period, i.e. the resistivity decreases (Fig. 7). The film thickness was less than the range of the ions. Unlike the case of epitaxially grown thin films having minimal grain boundaries, thick films have randomly oriented grains and correspondingly large grain boundaries. There are competing processes like creation and annihilation of charge carriers, modification of mean free path etc. which are to be understood both in the grains and grain boundaries. Local excitations due to irradiation cause the mean free path to decrease contributing to increase of the resistivity. Decrease of resistivity in thick films may be due to the increase in

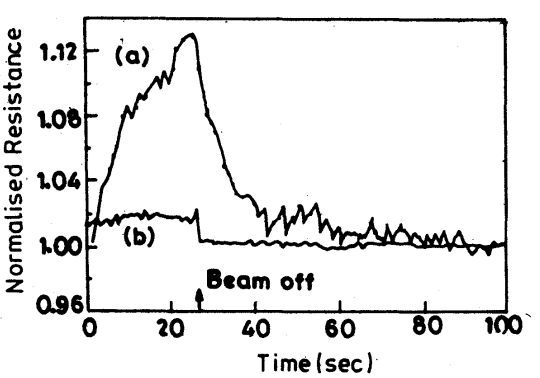

Fig. 6 Dynamic study with crystalline thin film during irradiation with 100 MeV oxygen ions

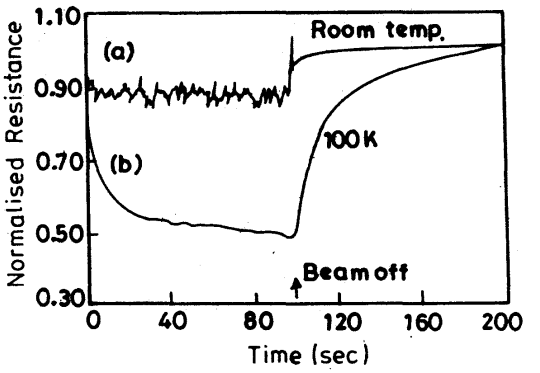

Fig. 7 Dynamic study with thick film (~10μm) during irradiation with 100 MeV oxygen ions

charge carriers created at the insulating grain boundaries providing a path for current through the disjointed grains. Observation of a long relaxation time for the resistivity of thick film is difficult to understand. Charge carrier production and annihilation cannot account for the long time scales (~100 sec) of post irradiation by diffusion of oxygen ions physically displaced by high energy beams. In a 123 system the apical and plane oxygen are far more stably bonded than the chain oxygen. The relaxation time of the thermally disordered chain oxygen at room temperature has been reported[49] to be of the order of hours. Short time scale of a few seconds for equilibration observed in our experiment is due to far from equilibrium state created by irradiation induced oxygen displacement/disorder. High energy ion beams, contrary to thermal excitation cause local excitations through electronic interaction processes displacing the plane and apical oxygen in addition to the chain oxgyen. The slow recovery of resistivity at low temperature compared to room temperature also points towards the recovery due to the oxygen diffusion. The abrupt rise and fall of resistivity on switching the beam off takes place because of relaxation of the system from a highly non-equilibrium state. This feature, prominent only at room temperature, indicates that phonons which scatter the charge carriers are involved in relaxation.

Colossal Magneto Resistance (CMR)

Colossal magneto resistance (CMR) in perovskites occurs only at large (several tesla) magnetic field and low temperature which restricts the applicability of these

materials considerably. It is required to achieve large magnetoresistance (MR) at low fields and at room temperature. Attempts are being made to engineer the appropriate material to achieve this objective. Studies are being made on superlattices involving magnetite layers, polycrystalline samples etc.[50-51]. Studies[52] on this subject emphasize that extended defects such as grain boundaries should have significant effect on the magnetotransport since internal interfaces are invariably associated with strain fields, and the magnetism and transport in manganites are linked to the bond properties. It is found[53-54] that low energy (keV) ion implantation causes significant changes in the transport behaviour of manganites but since the ion remains in the film it has non-uniform depth profile in the film. High energy (90 MeV) oxygen ion irradiation[55] of epitaxial LCMO thin film has been used to study the structural magnetization and magnetotransport properties in the fluence range of 10^{11} - 10^{14} ions/cm^2. The oxygen ions have low S_e value which produce point defects. SHI produced columnar defects generate compressive stress in the film. Its effect on transport properties needs to be investigated.

7 Polymer

Irradiation of polymers was known to just produce carbonization, which was considered as destruction. However, now it is realized that in polymers both productive and destructive radiation induced chemical reactions can coexist. Radiation induced reconstructive phase changes occur. In certain cases new carbonaceous material is formed with enhanced electrical conductivity. Enhanced electrical properties by several orders of magnitude have been observed. Ion beams can modify in a controlled way molecular structure in polymers leading to changes in their chemical, electronic electrical, tribiological and optical properties.

Ionization trail produced by SHI causes bond cleavages and free radicals produced at one site react in a molecular site of a different type from their original site. These are responsible for most of the chemical transformations observed in polymer films: chain scission, crosslinking and double and triple bond formation. Irreversible cleavages of bonds within the macromolecule produce volatile species.

The structural modifications in polymers depend on S_e and ion fluence. At low fluence, small value of S_e produces decrease in free volume i.e. densification occurs. This hinders dopant penetration giving surface sealing. Beyond the threshold S_e value SHI produces zone of reduced density along its trajectory (ion track).

Single ion track on selective etching produces micro-filters which find application in biomedical fields capable of filtering bacteria and possibly cancer cells. These tracks can be transformed into electronically active elements in nanoscopic devices by appropriate doping, i.e. filling the pores produced by etching the tracks with appropriate material.

The inner core of the track has a diameter of less than 10 nm. The track core is surrounded by the delta electrons having a range of 100-1000 nm. In polymers this track halo plays an important role since the delta electrons cause further damage such as strand breaks or crosslinks of polymer chains. Secondary reactions in the track halo occur on time scale of milliseconds to hours.

What happens in the material inside the track is a matter of great interest. It critically depends on the primary parameter, S_e. There are clusters formed, C_{60} gets synthesised in the column, possibly nanotubes are created etc.

SHI increases reflective index to permit optical guidance. It is seen that variation in reflective index depends on the parameters S_e and fluence and not on doping effect. This provides new possibilities for optimizing and controlling the loss in optical wave guides and channeling.

Particle Tracks Membrane (PTM) which provide cylindrical pores of uniform size can be modified to possess characteristics which depend on physical and/or chemical properties, according to environmental factors such as temperature, *p*H value, electric field etc. This provides possibilities of making sensitive sensors with SHI modified polymer materials.

Track Size and Structure in Polymer

The track diameter is a quantity of interest for the understanding of basic ion insulator interaction. These have been measured by scanning force microscopy and other surface morphology techniques. A novel approach has been used to determine the track diameters in polymers by on-line measurement of hydrogen loss

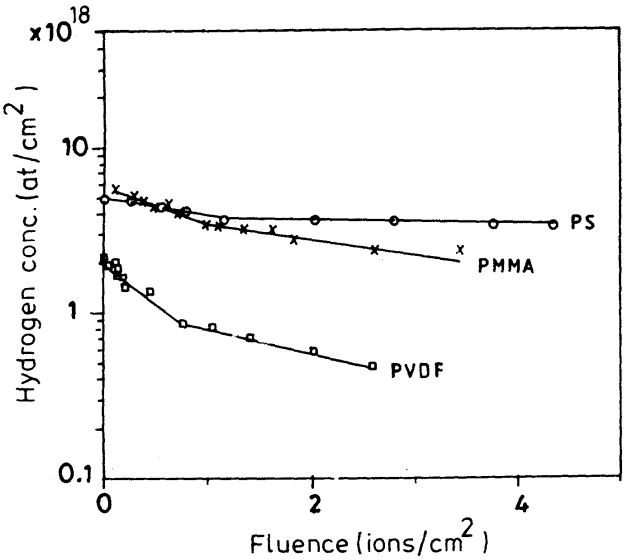

Fig. 8 Hydrogen loss *versus* fluence curve for 110 MeV ^{58}Ni bombarded on PS, PMMA and PVDF

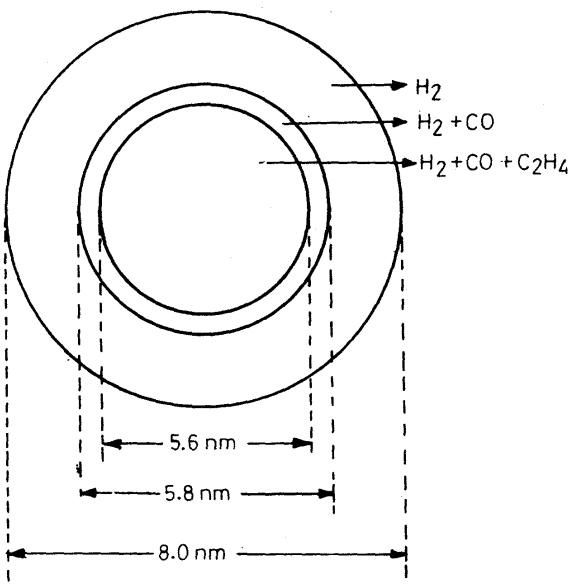

Fig. 9 Effective area of ion track damage due to evolution of H_2, CO and C_2H_4 gases

during ion irradiation by on-line elastic recoil detection analysis. Hydrogen atoms liberated by the breaking of the bonds combine to form hydrogen molecule, and being lightest gaseous molecule having high diffusivity, escape from the polymer causing reduction in H content. Thus incident ion along its path releases H from the cylindrical zone of damaged polymer. The variation of H content with ion dose is shown in Fig. 8. The track radius has been estimated by using the relation.

$$H(\varphi) = H_{in} \exp(-\rho.\phi)$$

where H_{in} represents initial content of H in the sample, ρ the cross-section of release of H and ϕ the ion fluence. The initial slope gives the cross-section of H release, which is equivalent to πr^2 with r as the track radius. The track radius in polyster and PVDF are estimated[56] as 3 nm and 6 nm respectively, which are consistent with other track radius measurements[57].

Evolution of gases from mylar was studied with an on-line quadrupole mass analyzer during irradiation with 180 Me V Ag ions. The gases evolved due to breakup of bonds were H_2, CO and C_2H_4. The track dimensions were evaluated by estimating the cross section of release of these gases. All the three gases are evolved from the region within a region of 6 nm (Fig. 9). The outer region between 6 and 8 nm correspond to H_2 emission[58]. The track structure has been studied with wide variation in S_e. It is found that the track core radius varies as $S_e^{0.55}$ which is surrounded by a halo caused by cross linking of macromolecules extending upto 100 nm in the case of u ions of 11.6 MeV/u energy[59].

8 Diamond Like Films

Diamond like carbon (DLC) thin films have been the subject of considerable attention because of their unique combination of properties, namely, extreme hardness, optical transparency, high electrical resistivity and chemical inertness. It is possible to vary these properties over a wide range of judiciously controlled film growth parameters, such as the deposition temperature, nature of source gas, hydrocarbon vs. hydrogen gas ratio etc. The properties obtained for these films are related to their microstructure, which involves various concentrations of hydrogen attached to carbon atoms at various SP^3, SP^2 and SP^1 sites. Energetic heavy ions can provide a handle for controlling or engineering these properties.

85 MeV nickel ions were used to study[60] the DLC thin films (1.2μm) deposited on polished Si (300mm) wafers by microwave discharge of acetylene (A type) and methane (M type) gases mixed with hydrogen. The films were irradiated to a dose of ~10^{14} ions cm^{-2}. The penetration depth of 85 MeV nickel ions is ~10μm and the electronic energy deposition at this energy is estimated to be ~1 keV/Å. The micro structure change associated with ion irradiation was found to be totally

different for the methane source (M^-) than in acetylene source (A^-) film. The films were characterized before and after irradiation using laser Raman (514 nm), Fourier transform IR (FTIR) and spectroscopic ellipsometry techniques. Raman spectra indicated evolution of fine micro graphite regions or disorder induced changes in the films. The FTIR spectra of M^- films after irradiation indicated increase in relative number of SP^2 sites compared with SP^3 sites. However, a relative decrease in SP^2 sites was indicated in A^- films. The spectral variation of the real part of the relative index, n, obtained by spectroscopic ellipsometry in the energy range 1.5-5.0 eV was found to be very different for M^- and A^- films. The value of n for M^- film decreases, whereas it increases for A^- films over the entire energy range on irradiation. The decrease of n, in M^- films on exposure to high energy ions can be explained by an increase in the graphite component of the DLC film (comprising of a diamond like component and a graphite component) via hydrogen release from the polymeric component. In A^- films, the increase in the value of n on irradiation can be explained in terms of the increased disorder and increase in the diamond like component. These observations are consistent with the Raman and IR spectra studies.

Hydrogen concentration and its depth profile in DLC films was also studied[61] using Elastic Recoil Detection Analysis (ERDA) with 85 MeV Ni ions. We found large changes (Fig. 10) in the hydrogen concentration in DLC films as a result of ion irradiation. Dischler *et al.*[62] had reported that DLC films annealed at 400°C retain a high proportion of diamond like SP^3 bonds which rapidly decrease with annealing temperature until, at 600°C, all the bonds are transferred into graphite - like SP^2 bonds. This is accompanied by hydrogen loss and a decrease in the transparency of these films. Under the conditions used for irradiation the temperature does not rise significantly but there may be change in SP^2-SP^3 ratio due to the electronic energy loss causing hydrogen loss.

Hydrogen profiling with heavy ions has the advantage that the scattering can safely be taken as pure Coulomb as in our case with 85 MeV nickel ions, and one does not require a reference H sample for calibration simplifying the experiment. Further, we can have simultaneous detection of hydrogen and carbon recoils providing relative number of hydrogen and carbon (Fig. 11).

In another experiment[63] dissociation kinetics of molecular hydrogen in microwave plasma and its influence on the hydrogen content in the diamond films was studied. The production rates of atomic hydrogen in the gaseous phase were evaluated to be 453, 1104

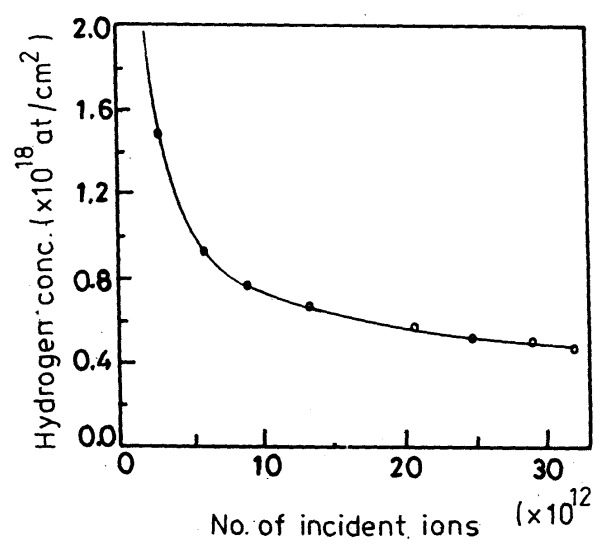

Fig. 10 Variation in the hydrogen ion concentration as a function of the number of incident ions determined by Elastic Recoil Detection Analysis (ERDA) using 85 MeV Ni ions

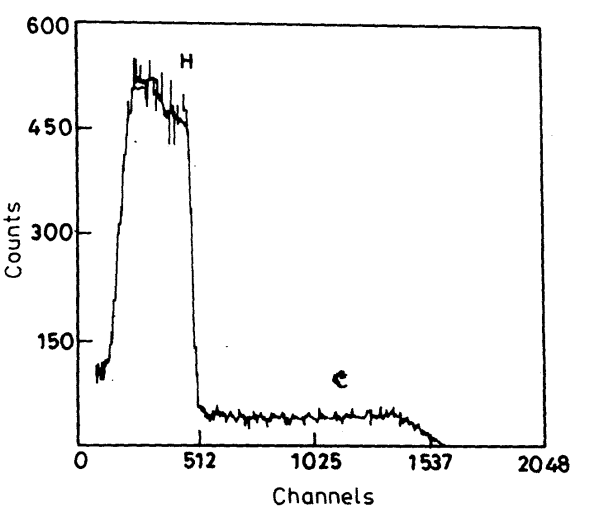

Fig. 11 Simultaneous detection of H and C in DLC films using the ERDA technique with 85 MeV Ni ion beam

and 1714 sec^{-1} at 20, 40 and 70 Torr respectively. A correlation was observed between the concentration of the atomic H in gaseous phase and the H content in the diamond thin film determined by ERDA.

9 SHI for Nanostructures

The columnar regions of modified materials produced by swift ions provide interesting possibilities of making nanostructured materials. Amorphized materials can be etched out and holes produced can be filled with material of interest to form appropriate structures as already mentioned earlier, but dimensions of etched holes are rather large from the nanostructure point of view. The situation becomes extremely interesting if the material of interest can be synthesized in the columnar regions by the swift ions. The diameter of columns is a few nanometers and thus modified material in these cylindrical regions embedded in the matrix of the original material is a nanostructure.

Magnetic Nanostructures

The magnetic properties of intermetallic alloys depend on their structural nature. The crystalline state is generally weakly magnetic but the amorphous state shows an enhanced magnetism. The precipitation of amorphous latent tracks in a crystalline matrix should thus, in principle, allow to control the magnetic properties at nanometer scale.

Ferromagnetic amorphous latent tracks have been observed[64] in YCO_2 thin films irradiated with 800 MeV/u ions. The diameter of the amorphous region has been estimated to be around 2 nm. This material is paramagnetic in crystalline form and ferromagnetic in amorphized forms. Thus SHI producing amorphized columns provides a way to configure ferromagnetic nanostructures in a non-magnetic crystalline matrix.

Nanocrystallites – Radiation Hard Materials

Nanocrystalline materials consist of small grains with diameter of a few tens of nanometers. The volume of interfacial regions can reach upto 40% if the grain size is <10 nm which is comparable to the diffusion length of the defects to interfaces, then all irradiation produced defects can readily annihilate in interfacial regions, instead of formation of defect clusters[65-66]. Effect of

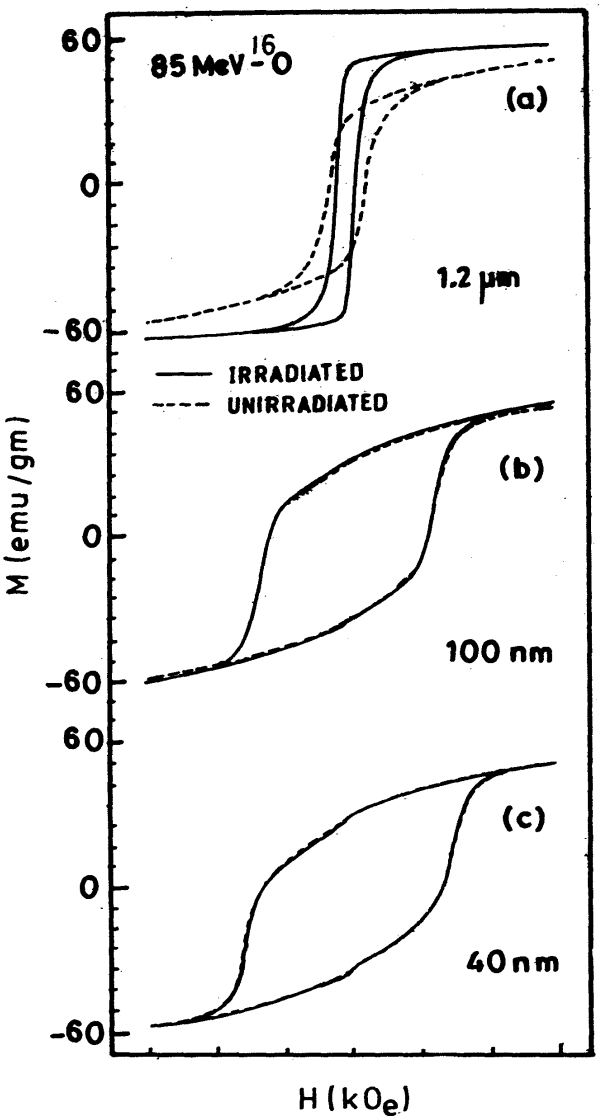

Fig. 12 Effect of heavy ion irradiation on hysterisis loops for micron sized and nano sized samples

SHI irradiation on magnetization behaviour of micro-sized and nano-sized powders of strontium ferrite ($SrFe_{12}O_{19}$) are investigated[67]. Significant changes in hysterisis loop features are observed (Fig. 12) after irradiation with 85 MeV ^{16}O ions in the case of micron-sized powders whereas no change is seen in the case of nano-sized powders. The stability of hysterisis loop of nano-sized powder to the irradiation of energetic ions shows that the nano-sized single domain particles are radiation hardened magnetic materials. The electronic stopping power of 85 MeV oxygen ions in $SrFe_{12}O_{19}$ is less than the calculated threshold value of S_e and thus latent tracks of amorphous material are not formed in

this case. The nature of defects produced is likely to be in the form of grain refinements along the ion trajectory into large grain boundary density.

10 Swift Heavy Ion Beam Analysis

The last decade has seen a rapid growth in materials technology involving electron beams, synchrotron radiation, neutrons and ion beams. Ions slow down in materials with little lateral scattering (unlike electrons), their velocity or energy at any point is a direct indication of the material depth traversed (unlike neutrons).

Fast ions probe the interfacial region between the regions covered by the very near surface examination techniques (optical, slow ion etc.) and bulk analysis methods (e.g. neutron). The effects associated with the penetration of ion beam in material are such that these methods are non-destructive. Further, they give rise to sensitivity to mass, charge and lattice position of constituent atoms, thus providing information that is largely unobtainable in other ways.

The analysis of elastic backscattering (EBS), commonly referred as Rutherford Back Scattering (RBS), of projectile ions provide depth profile information for heavy elements in low Z substrates. The second particle in the scattering process is the element being studied which kinematically has to recoil in forward direction. The analysis of these elastic recoils yields good depth resolution with high energy heavy ions. This technique, called elastic recoil detection analysis ERDA, is ideal for depth profiling of light elements in thin self supporting films. It was demonstrated[68] with carbon film with 100 MeV I ions using Si detector at 30° for determination of light elements C, N, O etc. that even the isotopes ^{12}C and ^{13}C could be separated in thin 500 nm self supporting foils. However, for thick films or even thin films on thick substrates it is difficult to get the resolution due to overlapping recoil energies. The use of state of the art nuclear detection techniques makes it possible[69] to circumvent the difficulty. The detection telescopé of ΔE and E detectors used for particle identification has been exploited[70] for simultaneous detection of H.C, N and O in DLC films and depth profiling of B and C in B implanted stainless steel[71].

ERDA is now a technique of choice for determining the depth distribution of hydrogen isotopes in the first several hundred nanometers of a surface. It can be exploited to monitor the changes in concentration of elements during ion irradiation as shown in an earlier section. SHI induced materials modifications seen as composition or depth profile changes can be measured *in situ* by ERDA[72].

11 Discussions

Ion beams in materials science and technology continue to provide new possibilities in sample characterization, analysis, development of materials, modification of the selective properties etc. Ion beam methods, provide a highly controllable set of tools which can be used for investigation systematically at the atomic level and ultimately controlled and exploited at the macroscopic level. The availability of large heavy ion accelerators has given rise to systematic studies of effects of SHI irradiation on various types of materials. For swift ions the electronic stopping power S_e (~ a few keV/Å) overwhelms the nuclear stopping power S_n (~a few eV/Å).

The conversion of the electronic energy into damage depends strongly on the material properties. The latent tracks in insulators and some other materials have been shown to have correlation of track radius (few nm) with S_e. This correlation can be explained using thermal spike concept with electron-photon coupling constant as the only free parameter. The fact that the columnar region can be produced in almost any material if the S_e is greater than the threshold value S_t for that material can also be explained with the thermal spike concept. When does the columnar region filled with the electronic energy qualify to become a latent track is a matter which requires wider understanding of the processes involved. It was known for a long time that latent tracks are not formed in metals but they do for thin metallic coating on thick substrates. Interface plays a significant role in changing electron-phonon coupling scenario. Metallic targets irradiated with GeV heavy ions showed the amorphised tracks. It is observed that S_e leads to various different types of effects depending on the nature of the target. SHI can produce defects of different types, can partially anneal defects originally present in the material, can create phase transformation (amorphization or crystallization), anisotropic growth of the material etc. Atomic size point defects can be produced if S_e is below threshold value S_t and

microstructure can be modified. The effects depend not only on the magnitude of S_e but also on fluence ϕ. Further, being the dynamic phenomena, effects produced depend on flux rate besides the most crucial factor which is the physics of the material. In some targets S_e does not seem to play any role in damage creation. The microscopic picture is visualized in terms of Coulomb explosion, thermal spike...? An appropriate theoretical model to understand various observations is yet to emerge. A viscoelastic model[73] has been proposed to interpret the plastic deformation observed in amorphous metallic alloys. The deformation is attributed to the relaxation of shear stresses coupled to the thermal expansion in cylindrical thermal spike. This concept of thermal spike seems to be applicable to most situations with significant success. However, it is worth emphasizing that the material modification induced by high density of electronic excitation in a columnar region is distinctly different from the thermal spike produced by laser beams.

There is a need to have more dynamic studies of the S_e induced effects. Since defect creation and annealing are transient processes probing of these phenomena needs on-line monitoring of the transient response of the system during irradiation under different conditions. Penetration of SHI in the material involves charge exchanges between the projectile ion and the target. There is mixing of energy levels of penetrating ions induced by the wake field produced by SHI. One has to understand transient strongly ionized cylinder produced by the ion passage. The life time of the ionized region is the crucial parameter which enters in thermal spike concept or Coulomb explosion picture. Auger electron emission from SHI irradiated targets can provide vital information. Electronic sputtering and *in situ* surface studies with STM, AFM, MFM associated with SHI irradiation provides information on an atomic level. A recent AFM study[74] with 830 MeV/u ions on graphite revealed sputtering craters from which carbon nanotubes emerged. The high energy ionoluminescence has the potential[75] to provide information on material structure during formation and evolution of radiation damages.

Nuclear particle track and modifications of materials have immense possibilities in the domain of microelectronics and nano-fabrications. By proper choice of ion species, energy and dose, nano beams can possibly be used for sputter removal of the material and dopants can be implanted for modification of electronic conduction at places of interest. In principle, complete dopant distribution can be written directly into the target material without the necessity of employing the conventional mask technology.

12 Acknowledgements

Discussions and help from Drs D Kanjilal, D K Avasthi and Prof N C Mishra regarding some sections of this paper is acknowledged. The financial support received from the Department of Science and Technology and the University Grants Commission in establishment of the facilities requires special mention which has made it possible for the user community to do research in this area. Major part of this review contains brief mention of the work done by the user community of NSC.

References

1 L C Northcliffe, R F Schilling *Nuclear Data Table* **A7** (1970) 233

2 J Dengler *et al. Hyperfine Interact* **70** (1992) 921

3 C Houpert, F Studer, H Pascard, J Y Fan and M Toulemond *Nucl Tracks Radiat Meas* **19** (1991) 85

4 A Meftah, J M Costantini, M Djebara, N Khalfaoui, J P Stoquert, F Studer and M Toulemonde *Nucl Instr & Meth* **B122** (1997) 470

5 F Studer, M Hervieu, J M Costantini and M Toulemonde *Nucl Instr & Meth* **B122** (1997) 449

6 A Barbu, H Dammaak, A Dunlop and D Lesueur *Ion Tracks in Metals and Intermetallic Compounds MRS Bull* (1995) 29

7 J Henry, A Barbu, B Leridon, D Lesueur and A Dunlop *Nucl Instr & Meth* **B67** (1992) 390

8 A Dunlop, G Jaskierowicz and S Della Negra *C R Acad Sci Paris* **325** (1997) 397

9 A Audouard, E Balanzat, J C Jousset, D Lesueur and L Thome *J Phys Cond Mater* **5** (1993) 995

10 G Szenes *Nucl Instr & Meth* **B116** (1996) 141

11 A Jain, S Loganathan, Jaipal, D Kanjilal and G K Mehta *Vacuum* **46** (1995) 369

12 S Srivastava, A Jain and D Kanjilal *Nucl Inst & Meth* **B101** (1995) 400

13 A Jain and S Srivastava *Thin Solid Films* **277** (1996) 128

14 S M H Ramos *et al. Nucl Inst & Meth* **B146** (1998) 462

15 Ajay Gupta *et al. Nucl Instr & Meth* **B146** (1998) 265

16 Ajay Gupta, A Paul, R Gupta, D K Avasthi *J Phys Cond Matter* **10** (1998) 9669

17 R Leguay *et al. Nucl Instr & Meth* **B122** (1997) 481

18 C T Reimann, W L Brown, D E Grosjean, M J Nowakowski *Phys Rev* **B45** (1992) 43

19 B U R Sundquist and R D Macfarlane *Mass Spect Rev* **4** (1985) 421

20 A Hedin, P Hakansson, M Salehpour, B U R Sundquist *Phys Rev* **B35** (1987) 1780

21 R E Johnson and B U R Sundquist *Phys Today* (March 1992) 28

22 L Calcagno, G Strazzula, M Fichera and G Foti *Rad Fe Lett* **76** (1983) 143

23 F Thibaudau, J Cousty, E Balanzat, S Bouffard *Phys Rev Lett* **67** (1991) 1582

24 B B Sharma, S R Gupta, R K Sharma, V Kumar, U Tiwari, P Sen and G K Mehta *MRS Spring Meeting San Francisco* (April 1995)

25 J Auleytner *Nucl Instr & Meth Phys Res* **B87** (1999) 124

26 D Zymierska *et al. Nucl Instr & Meth* **B146** (1998) 350

27 A M Narsale, V P Salvi, B M Arora, D Kanjilal and G K Mehta *J Appl Phys* **82** (1997) 4228

28 S T Chavan, P S Bhave, V N Bhoraskar and D Kanjilal *J Appl Phys* **78** (1995) 1

29 S T Chavan, S D Dhole and V N Bhoraskar *J Appl Phys* **78** (1997) 4805

30 S Arulkumaran, J Arokiaraj, M Udhayasankar, J Kumar and D Kanjilal *Rad Eff* (comm).

31 K L Bhatia, P Singh, M Singh, N Kishore, N C Mehta and D Kanjilal *Nucl Instr & Meth* **B94** (1994) 379

32 P Singh, K L Bhatia, N Kishore, M Singh, S K Malik and D Kanjilal *Jour Non-Crys Solids* **191** (1995) 146

33 T M Bhave, S V Bhoraskar, S Kulkarni and V N Bhoraskar *Jour App Phys* **29** (1996) 462

34 J P Singh, N C Mishra, R Singh, V Ganesan and D Kanjilal (to be published)

35 Ch Dufour, E Paumier and M Toulemonde *Nucl Instr & Meth* **B122** (1997)

36 P S Bhave and V N Bhoraskar *Nucl Instr & Meth* **B127/128** (1997) 383

37 S E Lofland, M X Huang, S M Bhagat, M Rajeshwari, T Venkatesan, D Kanjilal, L Senapati and G K Mehta *Phys Rev* **B51** (1995) 8489

38 S E Lofland *et al. Physica* **C267** (1996) 79

39 S G Kaplan, M Chen, H D Drew, M Rajeshwari, R Liu, T Venkatesan, D Kanjilal, L Senapati and G K Mehta *Physica* **C232** (1994) 174

40 A K Pradhan, P Chaddah, D Kanjilal, C Chen and B M Wanklyn *Phys Rev* **B53** (1996) 2269

41 A K Pradhan, B Chen, G Pindoria, K Nakao, N Koshizuka, D Kanjilal A J S Chowdhury and B N Wanklyn *Phys Rev* **B55** (1997) 11 129

42 S A Agnihotri, R H Bhawalkar, S Chandra, L Senapati, D Kanjilal and G K Mehta *Supercond Sci Tech* **15** (1992) 582

43 U Tiwari, N Sen, A K Bandyopadhyay, K Kanjilal and P Sen *Europhys Lett* **25** (1995) 705

44 N Sen, A Bandyopadhyay, O P Sen, U Tewari, D Varandani, V P S Awana and A V Narlikar *Solid State Comm* **82** (1992) 555

45 A Audouard, E Balanzat, J C Jousset, D Lesueur and L Thome *Jour Phys* **C5** (1993) 995

46 S Kloumunzer, M D Hou and G Schumacher *Phys Rev Lett* **57** (1986) 850

47 D Behera, N C Mishra and K Patnaik *Jour Supercond* **10** (1997) 27

48 N C Mishra, D Behera, T Mohanty, D Mohanta, D Kanjilal, G K Mehta and R Pinto *NIM* B (1999) (in press)

49 T Mohanty, A K Mohapatra, P K Samal, B N Dash, D B Behera, H P Mahapatra, S Mishra, N C Mishra, K Patnaik, L Senapati, D Kanjilal and G K Mehta *Indian Jour Phys* **69A** (1995) 29

50 C Kwon, K C Kim, M C Robson, J Y Gu, M Rajeshwari, T Venkatesan and R Ramesh *Jour Appl Phys* **81** (1997) 4950

51 N D Mathur, G Burnell *et al. Nature* **387** (1997)

52 S I Patil, R Shreekala, U Lanke, A Bhagwat and S B Ogale *Nucl Instr & Meth* **B114** (1996) 42

53 C H Chen *et al. App Phys Lett* **69** (1996) 3089

54 S B Ogale, K Ghosh, J Y Gu, R Shreekala, S R Shinde, M Downes, M Rajeshwari, R P Sharma, R L Greene, T Venkatesan, R Ramesh, R Bhate, S I Patil, Ravi Kumar, S K Arora and G K Mehta *Jour App Phys* **84** (1998)

55 S K Date, S R Shinde, L V Saraf, S B Ogale, R Kumar, S K Arora and G K Mehta *Jour Appl Phys* **83** (1998)

56 V K Mittal, S Loha and D K Avasthi *Rad Eff & Def in Solids* **147** (1997) 199

57 C Trautmann *Nucl Instr and Meth* **B105** (1995) 81

58 D K Avasthi, J P Singh, A Biswas and S K Basu *Nucl Instr & Meth* **B146** (1998) 504

59 P Apel *et al. Nucl Instr and Meth* **B146** (1998) 468

60 H C Barshilia, S Sah, B R Mehta, V D Vankar, D K Avasthi, Jaipal and G K Mehta *Thin Solid Films* **258** (1995) 123

61 D K Avasthi, D Kabiraj, Jaipal, G K Mehta, H C Barshilia, Somna Sah, B R Mehta and V D Vankar *Vacuum* **46** (1995) 633

62 B Dischler, A Bubenzer and P Koidl *Solid State Comm* **48** (1983) 3482

63 T Sharda, D S Mishra, D K Avasthi and G K Mehta (Comm)

64 M Ghidini, J P Nozieres, D Givord, A Lienard, B Gervais, E Dooryhee *Nucl Instr and Meth* **B107** (1996) 344; **B106** (1998) 250

65 T S Anderson *et al. Nucl Instr and Meth* **B124** (1997) 40

66 M Rose, A G Balogh, H Hahn *Nucl Inst and Meth* **B127/128** (1997) 119

67 S R Shinde, A Bhagwat, S I Patil, S B Ogale, G K Mehta, S K Datta, G Marest *Jour Magnet and Mag Materials* **186** (1998) 342

68 Jaipal, D Kabiraj and D K Avasthi *Nucl Instr and Meth* **A334** (1993) 196

69 B Roux, A Chevarier, N and Chevarier, B Wybourn, C Antoine, B Bonin, P Bosland and S Cantacuzene *Vacuum* **46** (1995) 629

70 D K Avasthi, D Kabiraj, A Bhagwat, G K Mehta, V D Vankar and S B Ogale *Nucl Instr and Meth* **B93** (1994) 480

71 D K Avasthi, D Kabiraj, A Jain and G K Mehta *Rev Sci Inst* **67** (1996) 3092

72 D K Avasthi, W Assmann, H Huber, H D Mieskes and H Nolte *Nucl Instr and Meth* (1998)

73 H Triankaus and A I Ryazanov *Phys Rev Lett* **75** (1995) 5072

74 L P Biro, B Szabo, G I Mark, J Gyulai, K Havancsak, J Kurti, A Dunlop, I Frey and H Ryssel *Nucl Instr and Meth* **B149** (1999) 1102

75 V A Skuratov, A Yu.Didyk, S M Abu Al Azm *Nucl Instr & Meth* **B94** (1994) 480